

Mechanism of Redox Reactions between $\text{SO}_3^{\bullet-}$ Radicals and Transition-Metal Macrocyclic Complexes: Oxidative Addition to the Ligand and Outer-Sphere Electron Transfer

S. K. Dutta and G. Ferraudi*

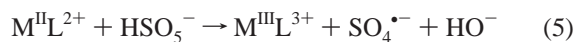
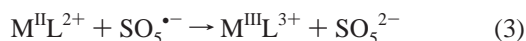
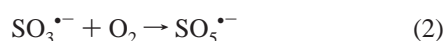
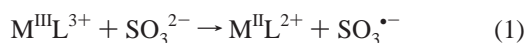
Radiation Laboratory, University of Notre Dame, Notre Dame, Indiana 46556

Received: September 28, 2000; In Final Form: January 16, 2001

Reactions of $\text{SO}_3^{\bullet-}$ radicals with complexes of Ni(II and I) and Cu(II and I) were investigated under anaerobic conditions. Reactions of CuCR^+ , Cu(TIM)^+ , and $\text{Ni}(\text{Me}_6[14]\text{dieneN}_4)^+$ with $\text{SO}_3^{\bullet-}$ radicals were investigated by time-resolved spectroscopy. The kinetics of the processes is in accordance with an outer-sphere electron-transfer mechanism. Intermediates with a ligand–radical nature were observed in $\text{SO}_3^{\bullet-}$ reactions with $\text{Cu}(2,9\text{-dimethyl-1,10-phenanthroline})_2^+$, $\text{Cu}(\text{Me}_6[14]\text{dieneN}_4)^{2+}$, NiCR^{2+} , or NiCRH_4^{2+} . Two products were isolated in the reaction of NiCR^{2+} with $\text{SO}_3^{\bullet-}$ radicals, one product with a sulfonated macrocycle and the other product with one additional double bond in the macrocycle. These products confirmed the attack of the ligand by $\text{SO}_3^{\bullet-}$ radicals and the formation of intermediates with a ligand–radical nature. A mechanism based on the oxidative addition of $\text{SO}_3^{\bullet-}$ radicals to the ligand accounts also for the kinetics of product formation.

Introduction

The reactions of $\text{SO}_3^{\bullet-}$ radicals with organic and inorganic compounds have commanded considerable interest because of the role of the radicals in grievous health and technological problems.^{1–12} Indeed, SO_3^{2-} , a biochemical source of such radicals and a product of industrial processes,^{7,8} has been recognized as a pollutant whose activity in the environment leads to numerous ails.^{8–10} Although the toxicological role of inorganic S(IV) and S(V) is now accepted, recent studies have shown that the mechanism by which these biological effects are manifested can be more complex than expected.^{11,12} In some of these studies, macrocyclic complexes of Ni(II) were used as catalysts of the aerobic oxidation of SO_3^{2-} and biochemical observations were rationalized in terms of the reaction mechanism in eqs 1–7.^{12,13}



An undefined initiator brings the metal complex, $\text{M}^{\text{II}}\text{L}$, to a higher oxidation state, $\text{M}^{\text{III}}\text{L}$, where it can oxidize SO_3^{2-} , eq 1. The propagation depends on the formation of $\text{SO}_5^{\bullet-}$ radicals when O_2 is present in the reaction medium, eqs 2, 5, and 6. Either $\text{SO}_4^{\bullet-}$ produced in eq 5 or $\text{SO}_5^{\bullet-}$ can oxidize $\text{M}^{\text{II}}\text{L}$, eqs 2 and 7, to reinitiate the cycle. This mechanism accounts for

the O_2 oxidation of SO_3^{2-} when simple transition-metal compounds, e.g., CoCl_2 and CuCl_2 , are used as catalysts. It also offers a good rationale for the damage of DNA by $\text{SO}_4^{\bullet-}$ and $\text{SO}_5^{\bullet-}$ radicals observed when Ni(II) macrocyclic complexes are used as catalysts of the aerobic oxidation of SO_3^{2-} .^{11,12}

In addition to the mechanism in eqs 1–7, related redox reactions of $\text{SO}_3^{\bullet-}$ radicals have been observed. Indeed, the tendency of $\text{SO}_3^{\bullet-}$ radicals to add to double bonds of organic molecules, free or coordinated to transition-metal ions, has been documented in several literature reports.^{1,14–17} It must be noted that identical sulfonated products may result from the oxidative addition of $\text{SO}_3^{\bullet-}$ radicals to the ligand or by SO_3 sulfonation of the ligand after the latter is formed via an outer-sphere electron-transfer reaction, eq 8. A process leading to the sulfonation of $[\text{Ru}(\text{NH}_3)_4(\text{phen})]^{3+}$, phen = 1,10-phenanthroline, by SO_3 has been discussed in a literature report.¹⁴

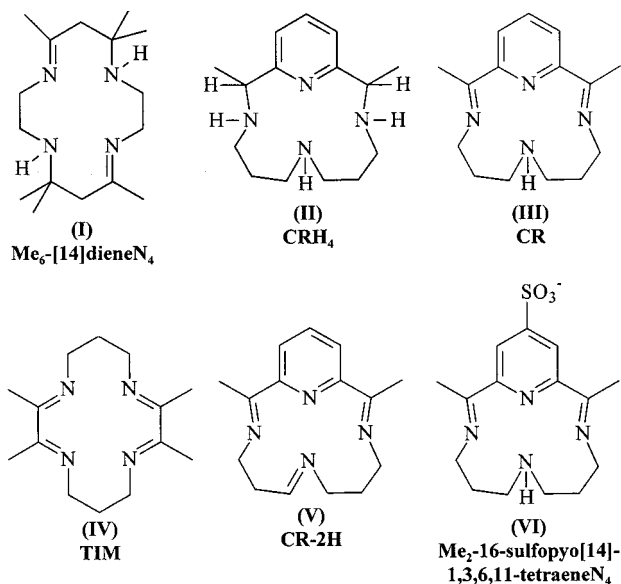


Redox reactions between $\text{SO}_3^{\bullet-}$ and transition-metal compounds with unsaturated macrocyclic ligands may proceed by either mechanism, i.e., an oxidative addition and/or an outer-sphere electron-transfer mechanism. To establish the relevance of these alternative mechanisms in redox reactions of $\text{SO}_3^{\bullet-}$ radicals with transition-metal compounds, we have studied the reactions of some macrocyclic complexes, **I–IV**, of Cu(II or I) and Ni(II or I) under anaerobic conditions.

Experimental Section

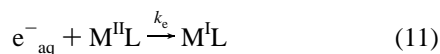
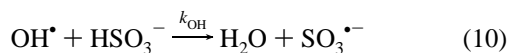
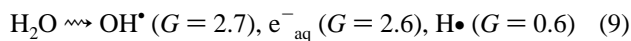
Materials. The perchlorate salts of various Ni(II) and Cu(II) complexes of the macrocyclic ligands **I–IV** were available from a previous work. $[\text{Cu}(\text{dmp})_2]\text{ClO}_4$ was prepared and purified by a literature procedure.¹⁸ The purity of the compound was evaluated by means of its absorption spectrum. Other chemicals were reagent grade and used without further purification.^{19,20}

Pulse Radiolysis. Pulse radiolysis experiments were carried out with a model TB-8/16-1S electron linear accelerator. The instrument and computerized data collection for time-resolved

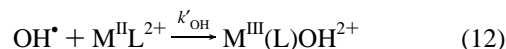


UV-vis spectroscopy and reaction kinetics have been described elsewhere in the literature.^{21a,b} Thiocyanate dosimetry was carried out at the beginning of each experimental session. The details of the dosimetry have been reported elsewhere.²¹ The procedure is based on the concentration of $(\text{SCN})_2^{\bullet-}$ radicals generated by the electron pulse in a N_2O -saturated 10^{-2} M SCN^- solution. In the procedure, the calculations of the dose are based on a $G = 6.13$ and an extinction coefficient $\epsilon = 7.58 \times 10^3 \text{ M}^{-1} \text{ cm}^{-1}$ at 472 nm for the $(\text{SCN})_2^{\bullet-}$ radicals.^{21a,b} In general, the experiments were carried out with a given dose that in a N_2 -saturated solution resulted in $(2.0 \pm 0.1) \times 10^{-6}$ M (dose $\approx 60 \text{ mJ g}^{-1} \text{ pulse}^{-1}$) to $(6 \pm 0.3) \times 10^{-6}$ M (dose $\approx 200 \text{ mJ g}^{-1} \text{ pulse}^{-1}$) concentrations of e^-_{aq} . Extinction coefficients of reaction intermediates were calculated with errors equal to or less than 10% as a function of dose. Liquids in the reaction cell were refreshed after each irradiation. In these experiments, solutions were deaerated with streams of the O_2 -free gas, N_2 or N_2O , required for the experiment. To prevent the catalyzed oxidation of SO_3^{2-} , the solutions were prepared by adding the proper amount of solid Na_2SO_3 to a deaerated solution containing the metallo complex and pH 6.5 buffer, i.e., 10^{-2} M $\text{H}_2\text{PO}_4^-/\text{HPO}_4^{2-}$. Although 20% of sulfite is in the form of SO_3^{2-} at pH 6.5, only deprotonated $\text{SO}_3^{\bullet-}$ radicals are produced at this pH. The mixture of HSO_3^- and SO_3^{2-} will be indicated as $\text{HSO}_3^-/\text{SO}_3^{2-}$ through the rest of the work.

In solutions deaerated with N_2 , reactions of pulse radiolytically generated solvated electrons ($G = 2.6$) and OH^\bullet ($G = 2.7$) radicals were respectively used for a nearly simultaneous formation of Ni(I) or Cu(I) complexes and $\text{SO}_3^{\bullet-}$ radicals, eqs 9–11.^{21b}



Reactions of $\text{SO}_3^{\bullet-}$ radicals with Ni(II) or Cu(II) complexes were investigated in solutions saturated with N_2O . Solvated electrons were first converted to OH^\bullet radicals, and the latter reacted quantitatively with SO_3^{2-} , eq 10. The concentrations of $\text{HSO}_3^-/\text{SO}_3^{2-}$ and $\text{M}^{\text{II}}\text{L}$ ions were adjusted to make insignificant any contribution of eq 12



to the experimental observations. To find the appropriate experimental conditions, tests were conducted with blanks that allowed the formation of either $\text{SO}_3^{\bullet-}$ radicals or $\text{M}^{\text{II}}\text{L}^+$ complexes to follow. The rate of formation of $\text{SO}_3^{\bullet-}$ radicals via eq 10 was investigated with solutions where $\text{M}^{\text{II}}\text{L}^{2+}$ was omitted. $\text{HSO}_3^-/\text{SO}_3^{2-}$ was replaced by 1% v/v $(\text{CH}_3)_3\text{COH}$ to trap OH radicals in blanks that were used for the investigation of the rate of $\text{M}^{\text{II}}\text{L}^+$ formation, eq 11. Several concentrations of $\text{M}^{\text{II}}\text{L}^{2+}$, equal to or smaller than 5.0×10^{-4} M, were used in these tests for a given concentration of $\text{HSO}_3^-/\text{SO}_3^{2-}$. In general, the generation of $\text{SO}_3^{\bullet-}$ radicals or $\text{M}^{\text{II}}\text{L}^+$ was accomplished in a period equal to or shorter than 0.3 μs , i.e., at least 10 times shorter than the lifetimes of the investigated reactions. Particular conditions used for time-resolved spectroscopy or in the investigation of reaction kinetics are given in the Results.

Steady-State Irradiations and Isolation of Reaction Products. Ion-exchange chromatographic separations on CM-Sephadex C-25 were also carried out under anaerobic conditions. N_2O -saturated solutions of the Ni(II) complexes and $\text{HSO}_3^-/\text{SO}_3^{2-}$ were prepared in gastight flasks by a procedure indicated above. The liquids in these flasks were placed in a Gammacell 200 and exposed to γ radiation for various periods. A spectrophotometer cell, attached to the side of the reaction flask, allowed to UV-vis spectral changes to be recorded without exposing the solution to air. In the separation of the various reaction products, the flask containing an irradiated solution was fastened to a deaerated chromatographic column. Empty spaces were purged with N_2 before the irradiated solution and elutant solutions, 0.1 M NaClO_4 , were run through the column. Calibrations of the radical concentrations produced in these irradiations were based on the concentration of $\text{Co}(\text{H}_2\text{O})_6^{2+}$ generated in the e^-_{aq} reduction of 10^{-3} M $\text{Co}(\text{NH}_3)_6^{3+}$ in a N_2 -saturated solution. In addition, the solution contained 10^{-1} M $(\text{CH}_3)_3\text{COH}$ for the scavenging of OH^\bullet radicals and was buffered at pH 6.5 with 10^{-2} M $\text{H}_2\text{PO}_4^-/\text{HPO}_4^{2-}$. Literature rate constants and pulse radiolysis experiments showed that $\text{Co}(\text{H}_2\text{O})_6^{2+}$ was produced with a yield, $G = 2.6$, equal to the yield of solvated electrons.²¹ The preparation and handling of the solutions for photochemical experiments were the same as those used in γ radiolysis. Photolytes were irradiated in a gastight cell for the spectrophotometric measurements with 1.0 and 0.2 cm optical paths.²² The cell with a capacity of ca. 5 cm^3 was described elsewhere in the literature. A 50 cm^3 reaction cell was used for the determination of gaseous products. Photolyzed solutions were frozen at -180°C , and the noncondensable gases were pumped off with a Toepler pump and analyzed in a Shimadzu GC-17A chromatograph provided with a RT-MSIEVES 13X (fused silica) column and a TC detector. Irradiations were carried out with light from a 360 nm Rayonet lamp. A light intensity $I \approx 10^{-4}$ einstein $\text{L}^{-1} \text{ min}^{-1}$ was measured with Parker's actinometer.²³

Isolated products from the steady-state irradiation were investigated by their ^1H NMR spectra. The spectra were recorded with a Varian Unity-Plus 300 MHz spectrometer of the Chemistry Department, University of Notre Dame.

Flash Photolysis. Flash photochemical irradiations at 351 nm were carried out with an apparatus described elsewhere.¹ Solutions for these experiments were prepared and handled by the same procedures as those described above.

Results

Experimental observations made on reactions of $\text{SO}_3^{\bullet-}$ radicals with various Ni and Cu complexes are summarized in

TABLE 1: Observed Reactions of $\text{SO}_3^{\bullet-}$ Radicals with Transition-Metal Complexes

reactant	$k \times 10^9,^a$ $\text{M}^{-1} \text{s}^{-1}$	$\epsilon^0(\text{II} \rightarrow \text{I}),^b$ V	$\epsilon^0(\text{III} \rightarrow \text{II}),^b$ V
CuCR^+	6.1 ± 0.3	-0.25	
CuTIM^+	13 ± 2	-0.38	
$\text{Ni}(\text{Me}_6[14]4,11\text{-dieneN}_4)^+$	2.9 ± 0.3	-0.97	
$\text{Cu}(\text{Me}_6[14]4,11\text{-dieneN}_4)^+$	RI ^c	-0.43	
$\text{Cu}(\text{dmp})_2^+$	RI	0.65	
NiCR_2^+	RI	-0.42	1.63
NiCRH_4^{2+}	RI	-0.99	1.43

^a Rate constants measured under conditions described elsewhere in the paper. ^b Typical redox potentials for the **II/I** and **III/II** couples in CH_3CN vs NHE. ^c Reaction intermediates were observed in flash photolysis and/or pulse radiolysis.

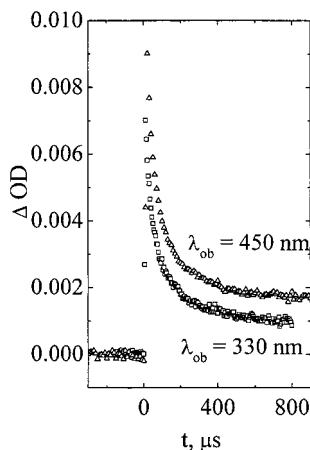
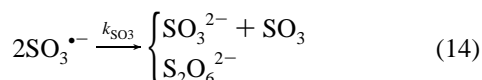
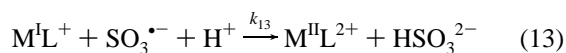


Figure 1. Oscillographic traces respectively recorded at 330 and 450 nm when $\text{Ni}(\text{Me}_6[14]4,11\text{-dieneN}_4)^+$ was pulse radiolytically generated in a N_2 -deaerated solution containing $2.0 \times 10^{-4} \text{ M Ni}(\text{Me}_6[14]4,11\text{-dieneN}_4)^{2+}$ and $2.0 \times 10^{-3} \text{ M HSO}_3^-/\text{SO}_3^{2-}$. The solution was buffered at pH 6.5 with $\text{H}_2\text{PO}_4^-/\text{HPO}_4^{2-}$.

Table 1. Literature values of the reduction potential $E^\circ = 0.73 \text{ V}$ vs NHE^{14,24,25} and the self-exchange rate constant $k_{\text{exc}} = 4 \text{ M}^{-1} \text{ s}^{-1}$ ^{14,26} were used for the $\text{SO}_3^{\bullet-}/\text{SO}_3^{2-}$ couple. In the following experiments at pH 6.5, 20% of sulfite is in the form of SO_3^{2-} . However, only $\text{SO}_3^{\bullet-}$ radicals are produced at this pH. The mixture of HSO_3^- and SO_3^{2-} will be indicated as $\text{HSO}_3^-/\text{SO}_3^{2-}$ through the rest of the work.

Reactions with Ni(I) and Cu(I) Reductants. In pulse radiolysis of $2.0 \times 10^{-4} \text{ M Ni}(\text{Me}_6[14]4,11\text{-dieneN}_4)^{2+}$ and $2.0 \times 10^{-3} \text{ M HSO}_3^-/\text{SO}_3^{2-}$, deaerated with N_2 , the product of the reduction exhibited bands at 450 and 330 nm that are characteristic of the Ni(I) complex. The spectrum of the Ni(I) complex disappeared via a process with second-order kinetics. A half-life period $t_{1/2} = 100 \mu\text{s}$ was recorded by following the decay of the 480 nm optical density of Ni(I) from its initial value, $\Delta\text{OD} = 7 \times 10^{-3}$. The decay of the spectrum leaves some residual Ni(I), Figure 1, which indicates that the reoxidation of the complex, eq 13, competes with radical-radical disproportionation and dimerization reactions, eq 14.²⁷



A rate constant $k_{13} = (2.9 \pm 0.3) \times 10^9 \text{ M}^{-1} \text{ s}^{-1}$ was calculated for the oxidation of Ni(I) by $\text{SO}_3^{\bullet-}$ radicals, eq 13, on the basis of the relationship of the initial to final ΔOD at 450 nm and

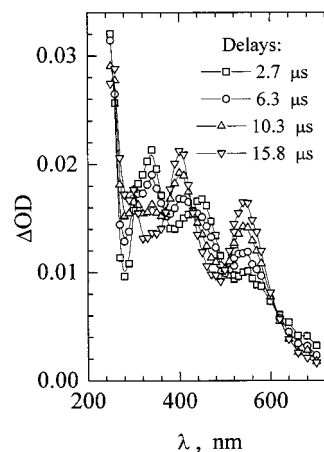


Figure 2. Transient spectra generated in pulse radiolysis of a $4.0 \times 10^{-5} \text{ M NiCRH}_4^{2+}$ and $4.0 \times 10^{-3} \text{ M HSO}_3^-/\text{SO}_3^{2-}$. The solution was buffered at pH 6.5 with $\text{H}_2\text{PO}_4^-/\text{HPO}_4^{2-}$ and deaerated with streams of N_2 .

the lifetime of the reaction. On the basis of the competition between eqs 13 and 14, the rate constant $k_{\text{SO}_3} = (8.0 \pm 0.9) \times 10^8 \text{ M}^{-1} \text{ s}^{-1}$ was calculated for the disproportionation/dimerization of the radicals, eq 14. The value agreed with a previous literature report.²⁷

Absorption bands at 450 and 330 nm were detected in pulse radiolysis of N_2 -deaerated solutions containing 2×10^{-5} or $4 \times 10^{-5} \text{ M NiCRH}_4^{2+}$, **II**, and 1×10^{-2} to $2 \times 10^{-3} \text{ M HSO}_3^-/\text{SO}_3^{2-}$ and buffered at pH 6.5, Figure 2. These absorptions were assigned to the reduction product of the Ni complex, NiCRH_4^+ . The rate constant $k \approx 5 \times 10^{11} \text{ M}^{-1} \text{ s}^{-1}$ was calculated for the reduction of NiCRH_4^{2+} from traces recorded at 450 and 330 nm. New absorption bands at 550 and 400 nm emerged later, in a slower process whose rate depended on the NiCRH_4^+ concentration, e.g., $t_{1/2} = 20 \pm 3 \mu\text{s}$ for $2 \times 10^{-5} \text{ M NiCRH}_4^{2+}$ and $t_{1/2} = 13 \pm 2 \mu\text{s}$ for $4 \times 10^{-5} \text{ M NiCRH}_4^{2+}$. While the rate of the OD growth increased with Ni(II) concentration, the final ΔOD at 550 and 400 nm remained nearly constant. These experimental observations revealed parallel reactions of $\text{SO}_3^{\bullet-}$ radicals with NiCRH_4^+ and NiCRH_4^{2+} . The competition between NiCRH_4^+ and NiCRH_4^{2+} for $\text{SO}_3^{\bullet-}$ radicals could not be resolved in favor of the NiCRH_4^+ reaction in experiments where smaller concentrations of NiCRH_4^{2+} were used for the investigation of the reaction rate. Therefore, no rate constant could be calculated for the reaction between NiCRH_4^+ and $\text{SO}_3^{\bullet-}$ radicals, eq 13.

The reaction of NiCR^+ , **III**, with $\text{SO}_3^{\bullet-}$ resembled that of NiCRH_4^{2+} in its competition with NiCR^{2+} for $\text{SO}_3^{\bullet-}$. In pulse radiolysis of a solution containing $4 \times 10^{-5} \text{ M NiCR}^{2+}$ and $2 \times 10^{-3} \text{ M HSO}_3^-/\text{SO}_3^{2-}$, buffered at pH 6.5 and deaerated with N_2 , the transient spectrum recorded several microseconds after the irradiation showed broad absorption bands at 450 and 320 nm. Such absorption bands suggested that NiCR^{2+} was simultaneously reduced by e^-_{aq} and oxidized by $\text{SO}_3^{\bullet-}$ radicals. Good linear least-squares fittings of ΔOD^{-1} vs time plots showed that the Ni(I) and Ni(III) products of the reaction disappeared with a second-order kinetics. Half-life periods $t_{1/2} = 120 \pm 5 \mu\text{s}$ for $\Delta\text{OD} = 0.004$ at the beginning of the reaction and $t_{1/2} = 13 \pm 1 \mu\text{s}$ for $\Delta\text{OD} = 0.03$ at the beginning of the reaction were measured from traces recorded at 450 nm. Since the Ni(III) species is formed later than the Ni(I) species by a slower process discussed elsewhere in the manuscript, an extinction coefficient $\epsilon = 1.9 \times 10^3 \text{ M}^{-1} \text{ cm}^{-1}$ was calculated at $\lambda_{\text{ob}} = 450 \text{ nm}$, i.e., where the main contribution to the spectrum is from the Ni(I) species. A rate constant $k \approx 4.4 \times 10^9 \text{ M}^{-1} \text{ s}^{-1}$ for the

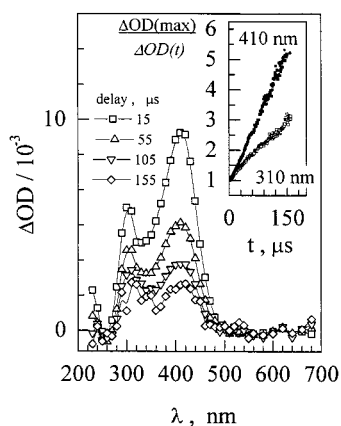


Figure 3. Transient spectra generated in pulse radiolysis of a N_2 -deaerated solution containing 2×10^{-4} M $Cu(Me_6[14]4,11\text{-diene}N_4)^{2+}$ and 4.0×10^{-3} M HSO_3^-/SO_3^{2-} . The inset shows the normalized optical density changes recorded at 410 and 310 nm. Note that the different slopes correspond to different rates at these two wavelengths.

reaction between Ni(I) and Ni(III) products was calculated by using the half-life periods. The concentrations of Ni(I) used in the calculation of the extinction coefficient and the rate constant were equal to the concentration of e^-_{aq} .

$Cu(Me_6[14]4,11\text{-diene}N_4)^+$ was produced in the irradiation of a N_2 -deaerated solution of $Cu(Me_6[14]4,11\text{-diene}N_4)^{2+}$, 2×10^{-4} M, containing 4×10^{-3} M HSO_3^-/SO_3^{2-} . The spectral transformations and reaction kinetics at different wavelengths indicate that oxidation of the Cu(I) product, eq 13, is mediated by a reaction intermediate, Figure 3. Also the oxidation of $Cu(dmp)^+$ by $SO_3^{\cdot-}$ radicals showed spectral changes and a kinetics in accordance with the formation of reaction intermediates. In solutions containing 4×10^{-5} M $Cu(dmp)^+$ and 2×10^{-3} M HSO_3^-/SO_3^{2-} , as a OH^{\cdot} scavenger, a bleach of the $Cu(dmp)^+$ optical density at 450 nm with $t_{1/2} = 5 \pm 0.2 \mu s$ coincided with a growth of the OD at 350 nm that is followed by a decay of the OD with $t_{1/2} = 20 \pm 3 \mu s$. This optical change at 350 nm indicates that a reaction intermediate with $t_{1/2} = 20 \mu s$ mediated the oxidation of the Cu(I) complex.

In reactions of 4×10^{-4} M $CuCR^{2+}$, **III**, or $CuTIM^{2+}$, **IV**, with e^-_{aq} , the reduced macrocycles $CuCR^+$ and $CuTIM^+$ were formed with $t_{1/2} < 1 \mu s$. These Cu(I) complexes disappeared in hundreds of microseconds by processes that were kinetically of second order. Since 4×10^{-3} M HSO_3^- totally scavenged OH radicals in less than $0.3 \mu s$, the disappearance of $CuCR^+$ and $CuTIM^+$ was ascribed to their respective reactions with $SO_3^{\cdot-}$ radicals, eq 13. The rate constants $k_{13} = (6.2 \pm 0.3) \times 10^9 M^{-1} s^{-1}$ for $CuCR^+$ and $k_{13} = (1.3 \pm 0.1) \times 10^{10} M^{-1} s^{-1}$ for $CuTIM^+$ were calculated from traces recorded at 675 and 720 nm where the corresponding extinction coefficients $\epsilon_{675} = 3.0 \times 10^3 M^{-1} cm^{-1}$ and $\epsilon_{720} = 7.2 \times 10^3 M^{-1} cm^{-1}$ were determined by means of the dose.

Time-Resolved Observations with $NiCR^{2+}$ and $NiCRH_4^{2+}$. Pulse radiolysis of N_2O -saturated 2×10^{-4} M $NiCR^{2+}$ and 2×10^{-3} M HSO_3^-/SO_3^{2-} , pH 6.5, produced transients with intense absorption bands at 290 and 240 nm and much weaker bands at longer wavelengths. The same spectral features were observed in the transient spectra recorded with a 2×10^{-4} M $NiCR^{2+}$ and 2×10^{-3} M HSO_3^-/SO_3^{2-} solution containing 3×10^{-3} M $Co(NH_3)_6^{3+}$, instead of N_2O , as a scavenger of e^-_{aq} . A reaction of the Ni(II) complex with $SO_3^{\cdot-}$ radicals accounts for the spectral changes during the first microsecond following the irradiation. Subsequent spectral changes, i.e., growth of 390 and 530 nm absorption bands and a partial decay of the optical

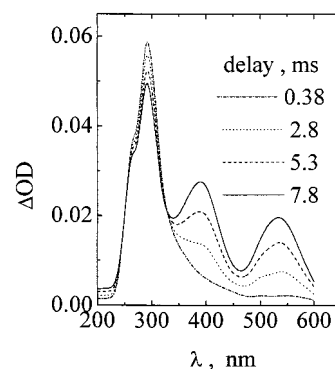


Figure 4. Transient spectra generated in pulse radiolysis of a N_2O -saturated solution containing 2.0×10^{-4} M $NiCR^{2+}$ and 2.0×10^{-3} M HSO_3^-/SO_3^{2-} . The solution was buffered at pH 6.5 with $H_2PO_4^-/HPO_4^{2-}$.

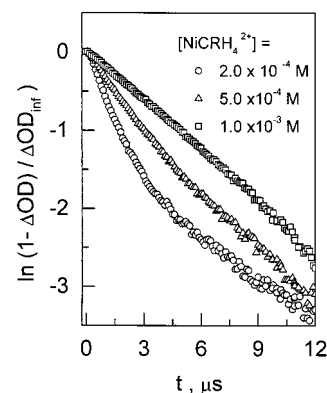


Figure 5. Initial processes in the oxidation of $NiCRH_4^{2+}$ by $SO_3^{\cdot-}$ radicals. The pulse radiolysis experiments were carried out with N_2O -saturated solutions containing 2.0×10^{-3} M HSO_3^-/SO_3^{2-} and (□) 1.0×10^{-3} M, (Δ) 5.0×10^{-4} M, and (○) 2.0×10^{-4} M $NiCR^{2+}$. The value of the OD change at the end of the reaction, $\Delta OD_{inf} \approx 0.042$ at $\lambda_{ob} = 390$ nm, was the same for the three concentrations of sulfite.

density near 300 nm, occurred over 20 ms, Figure 4. By comparison to literature spectra of Ni(III) complexes,²⁸⁻³⁰ an intermediate with spectral features $\epsilon = 1.3 \times 10^4 M^{-1} cm^{-1}$ at 390 nm and $\epsilon = 8.2 \times 10^3 M^{-1} cm^{-1}$ at 530 nm was characterized as a Ni(III) species. Because the conversion of this species to stable products was not completed within the maximum time range of the pulse radiolysis apparatus, the reaction kinetics could not be fully investigated. The stable products also have the spectra and reactivity of Ni(III) complexes. They survived more than 5 h in deaerated solutions and decayed to Ni(II) species that were investigated by using steady-state irradiations; see below.

A transient spectrum with bands at 550 and 400 nm was recorded in pulse radiolysis of N_2O -saturated 2×10^{-4} M $NiCRH_4^{2+}$ and 2×10^{-3} M HSO_3^-/SO_3^{2-} at pH 6.5. The growth of the absorption bands was slower than the scavenging of OH radicals by HSO_3^-/SO_3^{2-} , a reaction expected to have a half-life period $t_{1/2} \leq 0.3 \mu s$. In addition, the growth of the OD at 550 and 400 nm took place as a biphasic process with $t_{1/2} = 2.5 \pm 0.1 \mu s$ and $t_{1/2} = 30 \pm 0.3 \mu s$. Larger rates of the 550 and 400 nm OD growth were recorded with increasing $NiCRH_4^{2+}$ concentrations, $4 \times 10^{-5} M \leq [Ni(II)] \leq 1 \times 10^{-3} M$, but the ΔOD value at the end of the reaction remained nearly constant, Figure 5. These experimental observations showed that the reactions of $SO_3^{\cdot-}$ with $NiCRH_4^{2+}$ and $NiCR^{2+}$ have a similar mechanism.

Reactions with Ni(II) and Cu(II) Complexes. To study the Ni(III) products lasting a long time in solution, $SO_3^{\cdot-}$ radicals

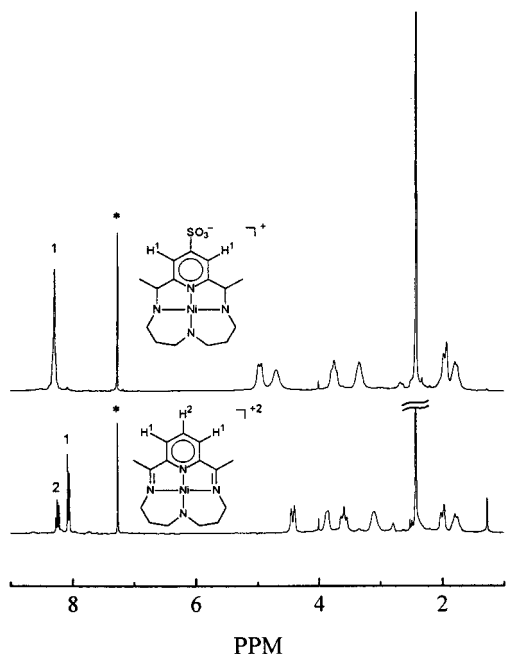
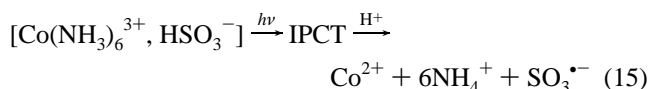


Figure 6. NMR spectra of Ni(Me₂-16-sulfopyo[14]-1,3,6,11-tetraeneN₄)⁺ (top) and NiCR²⁺ (bottom) recorded in CDCl₃ with 5% Cl₃-CCOOD.

were generated in γ radiolysis of N₂O-saturated solutions containing NiCR²⁺, 1×10^{-3} M, HSO₃⁻/SO₃²⁻, 1×10^{-2} M, and buffered at pH 6.5 with H₂PO₄⁻/HPO₄²⁻. Two stable Ni(II) products were isolated via anaerobic ion-exchange chromatography after the decay of the Ni(III) species, typically 24 h after the irradiation. These products were identified by their elemental analyses and UV-vis and NMR spectra, Figure 6. The spectral properties and elemental analysis of one product, isolated as a bright yellow powder, coincide with one known in the literature reports by the abbreviated name Ni(CR-2H)²⁺, **V**.²⁸ A second product, a dark yellow powder, was identified on the same experimental basis as Ni(Me₂-16-sulfopyo[14]-1,3,6,11-tetraeneN₄)⁺, **VI**, i.e., a sulfonated derivative of NiCR²⁺. The NMR spectra of the compound and the starting material, NiCR²⁺, are shown in Figure 6. In relative terms, the yield of Ni(CR-2H)²⁺ was less than half the yield of sulfonated product.

The effect of the metal on the oxidative addition of SO₃^{•-} radicals was investigated with several complexes. However, no redox reactions were observed with CuCR²⁺, Cu(Me₆[14]4,11-dieneN₄)²⁺, CuTIM²⁺, or Ni(Me₆[14]4,11-dieneN₄)²⁺ under the limiting condition indicated in the Experimental Section.

By comparison to the reactions described above, the reaction of NiCR²⁺ with SO₃^{•-} radicals provided experimental possibilities for a study of the reaction products. In addition to the steady-state radiolysis, photochemically generated SO₃^{•-} radicals were also reacted with NiCR²⁺. Steady-state, $\lambda_{\text{exc}} = 360$ nm, or flash, $\lambda_{\text{exc}} = 351$ nm, irradiations of the ion pair between Co(NH₃)₆³⁺, 5.0×10^{-3} M, and HSO₃⁻/SO₃²⁻, 5.0×10^{-2} to 1.25×10^{-2} M, were used for the photochemical generation of SO₃^{•-} radicals. Flash photolysis revealed the formation of SO₃^{•-} radicals according to eq 15,



where IPCT is the ion-pair charge-transfer excited state. The UV-vis spectral changes recorded in γ radiolysis and at the

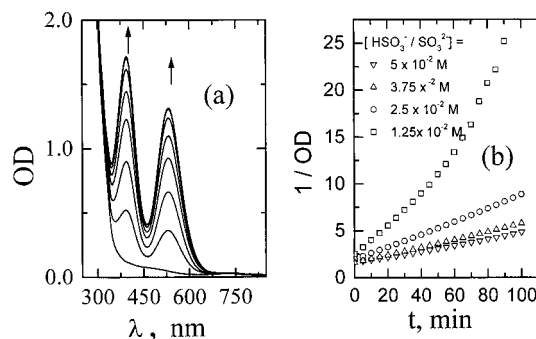


Figure 7. Spectra showing the formation of Ni(III) species (a). The spectra were recorded after consecutive 5 min irradiations in γ radiolysis of a N₂O-saturated solution containing 2.0×10^{-3} M NiCR²⁺ and 2.0×10^{-3} M HSO₃⁻/SO₃²⁻ and buffered at pH 6.5 with H₂PO₄⁻/HPO₄²⁻. In (b), inverse plots of the 530 nm optical density vs t show the disappearance of the Ni(III) species. The key in the figure gives the concentrations of HSO₃⁻ for each curve.

end of the time scale in pulse radiolysis were the same as those observed in steady-state and flash photolysis of NiCR²⁺ solutions containing Co(NH₃)₆³⁺ and HSO₃⁻/SO₃²⁻ at the concentrations indicated above. This experiment verified that the radiolytic and photochemical methods for the generation of SO₃^{•-} gave analogous results. On a longer time scale than those of pulse radiolysis or flash photolysis, the spectra of the irradiated solutions showed a growth of absorption bands with $\lambda_{\text{max}} = 390$ and 530 nm, Figure 7a. The decay of the Ni(III) products of the steady-state photolysis exhibited a complex kinetics, Figure 7b. It approached a second-order kinetics with the higher HSO₃⁻/SO₃²⁻ concentrations used in these experiments, e.g., more than 3.0×10^{-2} M. Deviations from a second-order kinetics were observed in solutions with a lower HSO₃⁻/SO₃²⁻ concentration.

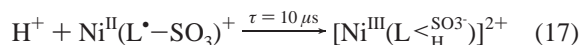
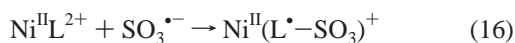
Discussion

The experimental evidence demonstrates that a large number of the investigated reactions between SO₃^{•-} radicals and coordination compounds of Ni(I or II) and Cu(I or II) have more complex mechanisms than an outer-sphere electron transfer. In these reactions, intermediates have been observed and/or their rate constants are unexpectedly large for an outer-sphere electron-transfer mechanism. These processes will be given special consideration after the discussion of the simpler outer-sphere electron-transfer reactions.

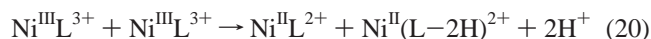
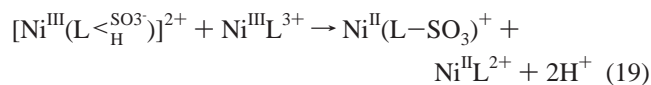
Outer-Sphere Electron-Transfer Reactions of SO₃^{•-}. By contrast to processes with a more complex mechanism, the oxidation of Ni(Me₆[14]4,11-dieneN₄)⁺, CuCR⁺, and CuTIM⁺ by SO₃^{•-} radicals produced no reaction intermediates in time-resolved experiments. Also, the reaction rate constants in Table 1 deviate by less than 20% from the rate constants calculated for an outer-sphere electron-transfer mechanism with literature potentials and self-exchange rate constants.^{14,20,24-26} In the absence of evidence to the contrary, it can be considered that these reactions proceed by such a mechanism.

Oxidative Addition Reactions of SO₃^{•-}. The oxidative sulfonation of the macrocyclic ligand was confirmed in reactions of NiCRH₄²⁺ and NiCR²⁺ with SO₃^{•-} radicals. Indeed, the sulfonated product that was isolated in the reaction of NiCR²⁺ with SO₃^{•-} is indicative of a process proceeding through the addition of the radical to the ligand. It is possible that the outer-sphere electron-transfer reactions between these compounds and SO₃^{•-} radicals are too slow to compete with oxidative additions to the macrocycle. Indeed, the negative redox oxidation

potentials of the M(II/III) couples in Table 1 and the small self-exchange rate constant of the $\text{SO}_3^{\bullet-}/\text{SO}_3^{2-}$ result in rate constants $k \ll 10^2 \text{ M}^{-1} \text{ s}^{-1}$ for an outer-sphere mechanism. The rapid formation of intermediates from the addition of the radical to the ligand suggests that this mechanism could be less kinetically impeded than the outer-sphere electron transfer. The absorption spectrum of the first intermediate generated in reactions of NiCR^{2+} , Figure 4, has features that would be expected for a Ni(II) ligand–radical. Indeed, absorptions between 300 and 400 nm were previously observed in reactions where OH^{\bullet} radicals add to pyridine derivatives and to the azine group of the CR ligand in complexes of Cu^{II} , Co^{II} , and Co^{III} .²⁹ In addition, the absorption spectrum and chemical properties of the second and longest lived intermediate are in accordance with those expected for Ni(III) macrocyclic complexes.^{30–32} It is possible to rationalize, therefore, the conversion of the first intermediate into the second in terms of an intramolecular electron transfer, i.e., one that is hampered by a large Marcus reorganization energy. The formation of the reaction intermediate and its conversion to a long-lived Ni(III) product are represented in eqs 16 and 17.



In eq 16, L is CR or CRH_4 and $\text{L}-\text{SO}_3^{\bullet-}$ is a coordinated ligand–radical. The intramolecular displacement of charge produces a long-lived Ni(III) species that precedes the formation of Ni(II) products on a time scale $t > 10^2 \text{ ms}$, eq 17. A decrease of the Ni(III) rate of decay with $\text{HSO}_3^-/\text{SO}_3^{2-}$ concentration can be accounted for by a reversible sulfonation of the ligand, eq 18, while equilibrated Ni(III) species disproportionate by rate-controlling reactions with a second-order kinetics, eqs 18–20.

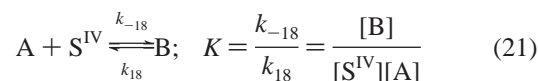


In reactions where the $\text{HSO}_3^-/\text{SO}_3^{2-}$ concentration was above $3.0 \times 10^{-2} \text{ M}$, the relaxation of the equilibrium, eq 18, appears to be fast in relation to the rate of eqs 19 and 20, Appendix. The ratio of the rate constant to the extinction coefficient, $k_{\text{ob}}/\epsilon \approx 3.1 \times 10^{-2} \text{ cm s}^{-1}$ at $\lambda_{\text{ob}} = 530 \text{ nm}$, was calculated under this approximation.³³ If one assumes that the Ni(III) products have similar extinction coefficients, the ratio of product yields found in steady-state irradiations suggests that $k/\epsilon \approx 2.3 \times 10^{-2} \text{ cm s}^{-1}$ for eq 19 and $kK/\epsilon \approx 7.8 \times 10^{-3} \text{ cm s}^{-1}$ for eq 20 at $\lambda_{\text{ob}} = 530 \text{ nm}$. The observed deviations from a second-order kinetics are accounted for if the rate of relaxation of the equilibrium, eq 18, approaches the rate of eqs 19 and 20, Appendix.

The disparate behavior of NiCR^{2+} and CuCR^{2+} , the former undergoes oxidative addition and the latter is unreactive or reacts slowly with $\text{SO}_3^{\bullet-}$ radicals, is suggestive of some activation of the macrocycle by Ni(II). Such activation could be dependent on the oxidation state of the metal. Indeed, $\text{Cu}(\text{dmp})_2^+$ and $\text{Cu}(\text{Me}_6[14]4,11\text{-dieneN}_4)^+$ appear to undergo oxidative additions while $\text{Ni}(\text{Me}_6[14]4,11\text{-dieneN}_4)^+$ is oxidized by $\text{SO}_3^{\bullet-}$ by way of an outer-sphere mechanism.

Appendix

Equations 18–20 can be condensed in the following equations:



In one experimental limit, the equilibration between A^+ and B, eq 21, is faster than the rate of consumption of A^+ and B via eqs 22 and 23. The combined decay of the Ni(III) species will be kinetically of second order with a rate constant $k_{\text{ob}}/\epsilon = (k_{19} + k_{20}K[\text{S}^{\text{IV}}])/(1 + K[\text{S}^{\text{IV}}])^2$ that includes the equilibrium constant, K , and the total concentration of sulfite, $[\text{S}^{\text{IV}}]$. Good linear least-squares fitting to plots of OD^{-1} vs t with $[\text{S}^{\text{IV}}] \geq 1.25 \times 10^{-2} \text{ M}$ were made under the approximation that the extinction coefficients of the Ni(III) complexes A and B were close, i.e., $\Delta\text{OD} = \epsilon_{\text{A}}[\text{A}] + \epsilon_{\text{B}}[\text{B}] \approx \epsilon([\text{A}] + [\text{B}])$.³³ An approximate value of the association constant $K \approx 2.1 \times 10^2 \text{ M}^{-1}$, $2k_{19} = (4.8 \pm 0.8) \times 10^{-4} \text{ M}^{-1} \text{ s}^{-1}$, and $k_{20} = (1.1 \pm 0.6) \times 10^{-3} \text{ M}^{-1} \text{ s}^{-1}$ were calculated for $\text{L} = \text{CR}$ from the dependence of tk_{ob} on $[\text{S}^{\text{IV}}]$.

Another experimental limit results when the rate of the equilibrium relaxation, eq 21, is comparable to the rate of consumption of A and B via eqs 22 and 23. The integrated rate laws are

$$[\text{B}] = \frac{k_{18}^2 K [\text{S}^{\text{IV}}] [\text{B}]_{t=0} e^{-k_{18}t}}{(k_{18}^2 K [\text{S}^{\text{IV}}] + 2k_{19}k_{20}[\text{B}]_{t=0})(1 - e^{-k_{18}t})}$$

$$= [\text{B}]_{t=0} \left(1 - \alpha t + \frac{1}{2} \alpha \left(\alpha + \frac{2k_{19}k_{20}[\text{B}]_{t=0}}{K[\text{S}^{\text{IV}}]k_{18}} \right) t^2 \dots \right)$$

where

$$\alpha = k_1 + \frac{2k_{19}k_{20}[\text{B}]_{t=0}}{k_{18}K[\text{S}^{\text{IV}}]} \quad \text{and} \quad [\text{A}^+] \approx \frac{k_{18}[\text{B}]}{k_{19}[\text{B}] + k_{18}K[\text{S}^{\text{IV}}]}$$

In the integrated rate law for B, increasing concentrations of S^{IV} will make the overall process of a first-order kinetics.

Acknowledgment. The work described herein was supported by the Office of Basic Energy Sciences of the U.S. Department of Energy. This is contribution no. NDRL-4240 from the Notre Dame Radiation Laboratory. G.F. acknowledges support from the NSF, Grant INT97-26738. We also thank Dr. D. Meisel for helpful discussions of the manuscript.

References and Notes

- Gibney, C. S.; Ferraudi, G.; Shang, M. *Inorg. Chem.* **1999**, *38*, 2898.
- Connick, R. E.; Zhang, Y.; Lee, S.; Adamic, R.; Chieng, P. *Inorg. Chem.* **1995**, *34*, 4543.
- Connick, R. E.; Zhang, Y. *Inorg. Chem.* **1996**, *35*, 4613.
- Fronaeus, S.; Berglund, J.; Elding, L. I. *Inorg. Chem.* **1998**, *37*, 4939 and references therein.
- Brandt, C.; Fabián, I.; van Eldik, R. *Inorg. Chem.* **1994**, *33*, 687.
- Brandt, C.; van Eldik, R. *Chem. Rev.* **1995**, *95*, 119.
- Meyer, B. *Sulfur, Energy and Environment*; Elsevier Scientific Publishing Co.: Amsterdam, The Netherlands, 1977.
- Kaplan, D.; McJilton, C.; Luchtel, D. *Arch. Environ. Health* **1975**, *30*, 507.

- (9) Hayatsu, H.; Miller, R. C. *Biochem. Biophys. Res. Commun.* **1972**, *46*, 120.
- (10) Reed, G. A.; Curts, J. F.; Mottley, C.; Eling, T. E.; Mason, R. P. *Proc. Natl. Acad. Sci. U.S.A.* **1986**, *83*, 7499.
- (11) Muller, G. J.; Chen, X.; Dadiz, A. C.; Rokita, S. E.; Burrows, C. *J. Am. Chem. Soc.* **1992**, *114*, 6407.
- (12) Muller, G. J.; Hickerson, R. P.; Perez, R. J.; Burrows, C. J. *J. Am. Chem. Soc.* **1997**, *119*, 1501.
- (13) Coichev, N.; van Eldik, R. *Inorg. Chem.* **1991**, *30*, 2375.
- (14) Sarala, R.; Islam, M. A.; Rabin, S. B.; Stanbury, D. A. *Inorg. Chem.* **1990**, *29*, 1133.
- (15) Murray, R. S. *J. Chem. Soc., Dalton Trans.* **1974**, 2381.
- (16) Erben-Russ, M.; Bors, W.; Winter, R.; Saran, M. *Radiat. Phys. Chem.* **1986**, *27*, 419.
- (17) Ozawa, T.; Kwan, T. *Polyhedron* **1986**, *5*, 1531.
- (18) Hall, J. R.; Marchant, N. J.; Plowman, N. R. *Aust. J. Chem.* **1962**, *15*, 480.
- (19) Ferraudi, G.; Barrera, P.; Granifo, J.; Ham, J. H.; Rillema, P. D. *Inorg. Chem.* **1985**, *24*, 281.
- (20) Ronco, S.; Van Vlierberge, B.; Ferraudi, G. *Inorg. Chem.* **1988**, *27*, 3453.
- (21) (a) Hugh, G. L.; Wang, Y.; Schöneich, C.; Jiang, P.-Y.; Fesenden, R. W. *Radiat. Phys. Chem.* **1999**, *54*, 559. (b) G is defined as the number of molecules formed per 100 eV of radiation. For additional details see: Buxton, G. V.; Greenstock, C. L.; Hellman, W. P.; Ross, A. B. *J. Phys. Chem. Ref. Data* **1988**, *17*, 513. (c) Feliz, M. R.; Ferraudi, G. *Inorg. Chem.* **1998**, *37*, 2806.
- (22) Ferraudi, G. *Inorg. Chem.* **1980**, *19*, 438.
- (23) Hatchard, C. G.; Parker, C. A. *Proc. R. Soc. London, Ser. A* **1956**, *235*, 518.
- (24) Das, T. N.; Huie, R. H.; Neta, P. *J. Phys. Chem. A* **1999**, *103*, 3581.
- (25) Huie, R.; Neta, P. *J. Phys. Chem.* **1985**, *89*, 3918.
- (26) Note that values of k_{xchg} on p 2904 of ref 1 are multiplied by a 10^7 factor due to a typographical error. The actual value is $k_{\text{xchg}} = 6 \text{ M}^{-1} \text{ s}^{-1}$ instead of the reported one. This value, as was indicated in ref 1, is in good agreement with one, $k_{\text{xchg}} = 4 \text{ M}^{-1} \text{ s}^{-1}$, previously calculated by Stanbury et al.¹⁴
- (27) (a) Eriksen, T. *J. Chem. Soc., Faraday Trans. 1* **1974**, *20*, 208. (b) Buxton, G. V.; McGowan, S.; Salmon, G. A.; William, J. E.; Wood, N. D. *Atmos. Environ.* **1996**, *30*, 2483. (c) Hug, G. *Optical Spectra of Nonmetallic Inorganic Transient Species in Aqueous Solutions*; National Standard Reference Data Series; Natl. Bur. Stand. NSRDS-NBS 69; National Bureau of Standards: Washington, DC, 1981.
- (28) Barefield, K.; Lovecchio, F. V.; Tokel, N. E.; Ociai, E.; Busch, D. H. *Inorg. Chem.* **1972**, *11*, 283.
- (29) Geiger, D. K.; Ferraudi, G. *Inorg. Chim. Acta* **1986**, *117*, 139.
- (30) Morliere, P.; Patterson, L. K. *Inorg. Chem.* **1982**, *21*, 1837.
- (31) Morliere, P.; Patterson, L. K. *Inorg. Chem.* **1981**, *20*, 1458.
- (32) Maruthamuthu, P.; Patterson, L. K.; Ferraudi, G. *Inorg. Chem.* **1978**, *17*, 3157.
- (33) Since the Ni(III) species are in equilibrium, ΔOD is a measure of the total Ni(III) concentration and the rate constant is for the overall rate of Ni(III) decay.